

Supplemental data:

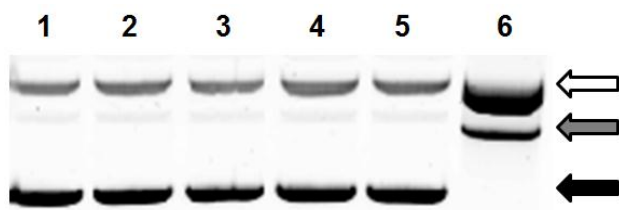
## **Cytotoxicity and DNA cleavage with core-shell nanocomposites functionalized by a KH domain DNA binding peptide**

*Remon Bazak, Jan Ressler, Sumita Raha, Caroline Doty, William Liu, M Beau Wanzer, Seddik*

*Abdel Salam, Samy Elwany, Tatjana Paunesku, and Gayle E Woloschak*

### **Activated non-functionalized nanocomposites cause DNA scission *in vitro***

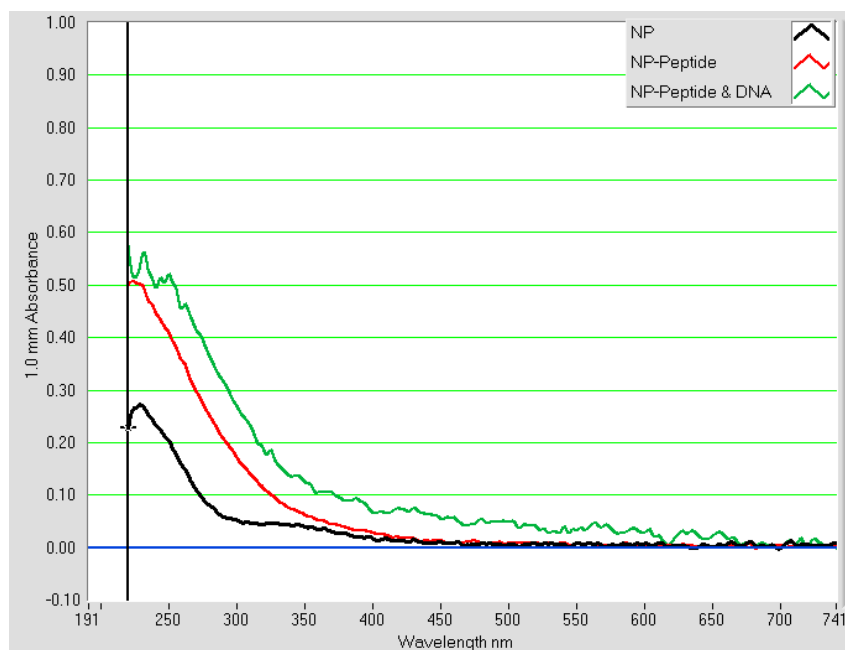
The core-shell nanocomposites were compared with pure TiO<sub>2</sub> nanoparticles for their capacity to induce DNA cleavage *in vitro* (Supplemental Figure 1) following excitation with white light. Nanoparticles were mixed with plasmid DNA in a 10 mM phosphate buffer, aliquoted and illuminated on ice with a quartz halogen lamp (Fiber Lite MI-150, Dolan Jenner), with transmittance of 20% at 400 nm, at a maximum intensity for 10 minutes. Under the illumination and concentration conditions used, only the core-shell nanocomposites produced sufficient DNA cleavage to form linearized plasmid DNA and an increased amount of nicked DNA (lane 6). This finding was in agreement with expectations based on work with the doped TiO<sub>2</sub> materials.<sup>(1)</sup> For example, presence of silver redirects the electrons from the conduction band of the TiO<sub>2</sub> toward silver because its Fermi level is below that of titanium,<sup>(1)</sup> and the electronic state energy of Fe is even lower than that of Ag. Therefore, doping TiO<sub>2</sub> with iron<sup>(2)</sup> decreases the band gap energy of nanoparticles, and similar effects have been found for TiO<sub>2</sub> particles with an Fe<sub>3</sub>O<sub>4</sub> core.<sup>(3)</sup>



**Supplemental Figure 1.** Plasmid DNA cleavage induced by illumination in the presence of 560 nM  $\text{TiO}_2$  nanoparticles (0.09 mg/ml  $\text{TiO}_2$ ) with a 5 nm diameter (lanes 3 and 4) or 560 nM, 6.5 nm diameter core shell  $\text{Fe}_3\text{O}_4@ \text{TiO}_2$  nanocomposites (0.18 mg/ml of  $\text{TiO}_2$ ) (lanes 5 and 6). Plasmid alone (lanes 1 and 2) or combined with nanoparticles or nanocomposites was separated into two aliquots, and one aliquot was left in the dark (lanes 1, 3, 5) while the other aliquot was illuminated with white light for 10 minutes (lanes 2, 4, 6). Supercoiled DNA (black arrow) is undamaged, relaxed DNA (white arrow) carries at least a single strand DNA cut, while linear plasmid DNA (gray arrow) has at least one double strand DNA break.

## Conjugation of KH peptide to nanocomposites changes their UV-vis spectra

The conjugation between the nanoparticles and the KH peptide was confirmed by UV-visible light spectroscopy using the NanoDrop ND-1000 Spectrophotometer (Supplemental Figure 2).

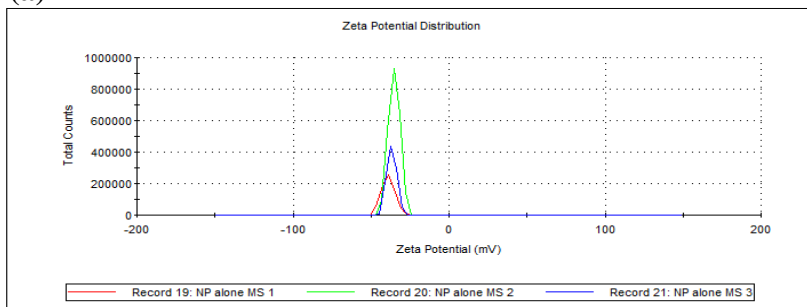


**Supplemental Figure 2:** UV-VIS absorbance spectra of nanocomposites with and without peptide coating and peptide and DNA coating. Prior to conjugation of ARS, peptide coated core-shell nanoparticles were examined by spectroscopy. The addition of KH-peptide to the nanoconjugate (red line) results in a red shift of absorption compared to the nanoconjugates alone (black line); the addition of DNA (cDNA of c-Myc gene) resulted in an even more pronounced red shift (green line).

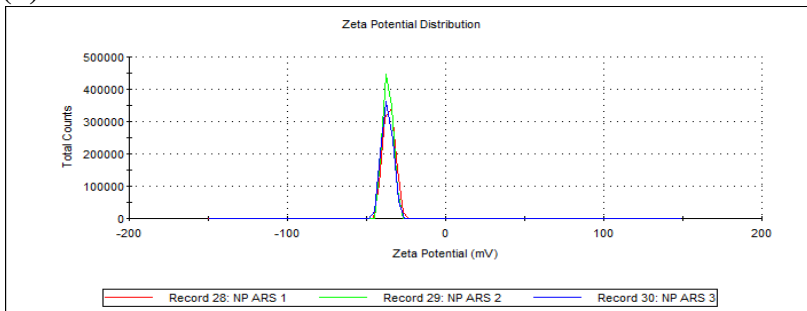
**Dynamic light scattering shows that presence of KH peptide does not significantly modulate zeta potential of nanocomposites**

Dynamic light scattering (DLS) was used to determine the zeta potentials of the bare nanoparticles, ARS coated nanoparticles, and KH-peptide-ARS coated nanoparticles (Supplemental Figure 3). Samples for DLS analysis were diluted 1:100 in distilled water and injected into clear, disposable capillary tubes (Malvern DTS1061). The zeta potentials were read in triplicate on a Malvern Zetasizer Nano. The zeta potentials of different samples were close to -35 in all cases (Supplemental Figure 3).

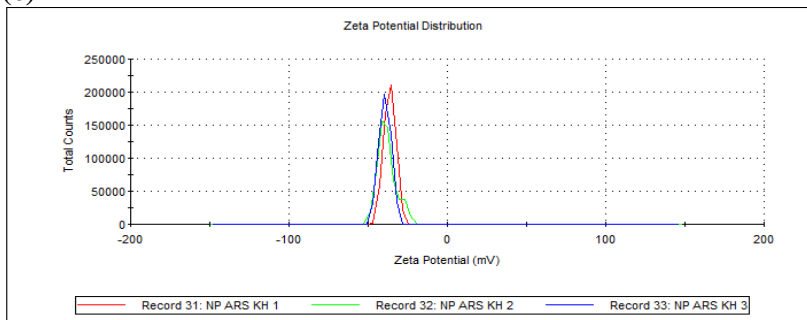
(a)



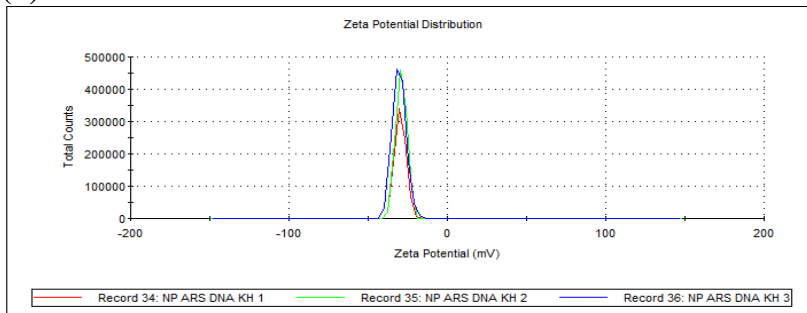
(b)



(c)



(d)



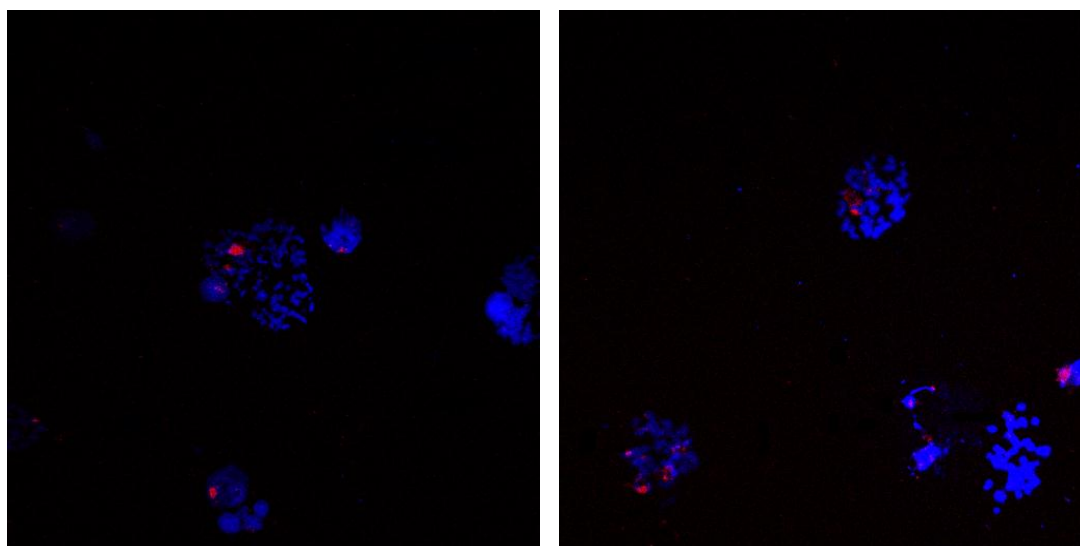
**Supplemental Figure 3. The zeta potentials of nanoparticles used in this study** (a) The zeta potential of bare core-shell nanocomposites was  $-37 \pm 1.96$ ; (b) for Alizarin coated nanocomposites it was  $-36.4 \pm 0.611$ ; for (c) ARS and KH-peptide coated nanocomposites  $-38.0 \pm 1.51$ ; and for (d) ARS, KH-peptide and DNA coated nanocomposites  $-29.7 \pm 0.611$ .

### **Preparation of NP-KH-DNA nanocomposites and fluorescence in situ hybridization (FISH)**

**Probe preparation:** A plasmid containing a DNA sequence complementary to c-Myc gene was obtained from GeneCopoeia (Catalog No. EX-Z2845-B09). The open reading frame length is 1365 base pair (bp); this plasmid was transfected into DH5 $\alpha$  E. coli, isolated using a Qiagen kit and the DNA fragment of myc cDNA isolated following a restriction digest and gel purification. This DNA was attached to the nanocomposites via dopamine linker. Conjugation between the free phosphate group and dopamine was done using the procedure described in Thermo Scientific Technical Tips. Briefly, in a 1.5 ml Eppendorf tube, 75  $\mu$ l of myc cDNA probe in water was mixed with 5  $\mu$ l of Dopamine (250 mM in 0.1 M imidazole) and 1.25 mg of 1-ethyl-3-(3-dimethylaminopropyl) carbodiimide (EDC). All reagents were purchased from Thermo Scientific. The reactants were then mixed gently and left at room temperature within the nitrogen hood for 10 minutes, after which 20  $\mu$ l of 0.1 M imidazole was added and the reactants were left for another 2 hours. 3 ml of the NP-KH peptide suspension (150  $\mu$ l of KH-peptide, 2 ng/ml + 80  $\mu$ l ARS, 10 mM) was then added and the entire mixture was incubated overnight.

**FISH:** Synchronized cells were collected at 30 hours after mitotic shake-off, when majority of them enters the M phase and fixed in methanol at -20°C. Chromosomes were drop cast onto slides permeabilized with Triton-X 100 in phosphate buffered saline (PBS), incubated in 20% glycerol in PBS and subjected to several freeze-thaw cycles. DNA was prepared for hybridization by exposure to 0.1 N HCL and washed in 2xSSC pH 7.0. Following an additional treatment with 50% Formamide in 2x SSC pH 7.0 slides were exposed to the "probe" prepared as

described and denatured in the same buffer. The probe consisted of nanoconjugates with their surface covered with a myc c-DNA probe and KH peptide. The sealed slides were exposed to 75°C for 2 minutes and moved to a 37°C humid chamber overnight. Slides were washed in 2xSSC and the nanoparticles were visualized by Alizarin red S stain, while the DNA was stained with Hoechst. The slides were examined at the Nikon C1si confocal microscope at Northwestern cell imaging facility.

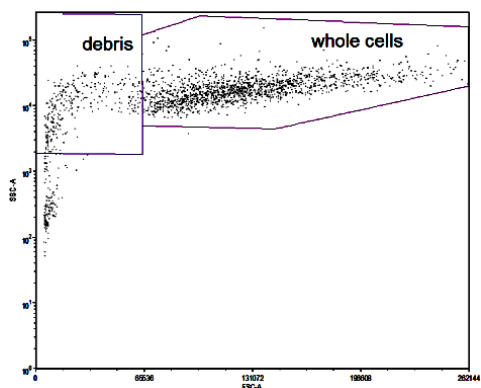


**Supplemental Figure 4.** FISH for c-Myc gene in RPMI2650 cell line.

The nanocomposites carrying a 1.3 kb cDNA for c-Myc gene and KH peptide were post-stained with Alizarin red S at the same time when the chromosomes were stained with Hoechst, immediately prior to imaging. Nanoparticles appear red because of ARS, while the DNA is stained blue. In most cells multiple copies of c-Myc gene are evident.

## Flow cytometry of cells treated with nanoconjugates

Flow cytometry demonstrated variable amounts of cell debris which appeared most abundantly after exposure to nanocomposites and UV illumination; for that reason we chose to include the debris data in our final analysis of these samples (Figure 4). A similar approach was used by others in the literature.<sup>(4)</sup>



**Supplemental Figure 5.** Flow cytometry gating applied on control cells is shown as an example of flow cytometry gates used to define the debris and whole cells. All flow cytometry results were analyzed identically, using these two gates—one for debris and one for whole cells as shown here. Subsequently, whole cells were segregated into live, apoptotic (early and late) or necrotic, according to the distribution of cells into non-fluorescent-live, and those fluorescent for annexin V (APC)-apoptotic, those with leaky cell membranes (Sytox blue)-dead, or both.

## References

1. Wodka D, Bielanska E, Socha RP, Elzbieciak-Wodka M, Gurgul J, Nowak P, et al. Photocatalytic activity of titanium dioxide modified by silver nanoparticles. *ACS Appl Mater Interfaces*. 2010 Jul;**2**(7):1945-53.
2. George S, Pokhrel S, Ji Z, Henderson BL, Xia T, Li L, Zink JJ, et al. Role of Fe doping in tuning the band gap of TiO<sub>2</sub> for the photo-oxidation-induced cytotoxicity paradigm. *J Am Chem Soc*. 2011 Jul;**133**(29):11270-8.
3. Yao KF, Peng Z, Liao ZH, Chen JJ. Preparation and photocatalytic property of TiO<sub>2</sub>-Fe<sub>3</sub>O<sub>4</sub> core-shell nanoparticles. *J Nanosci Nanotechnol*. 2009 Feb;**9**(2):1458-61.
4. Minervini F, Fornelli F, Flynn KM. Toxicity and apoptosis induced by the mycotoxins nivalenol, deoxynivalenol and fumonisin B1 in a human erythroleukemia cell line. *Toxicol In Vitro*. 2004 Feb;**18**(1):21-8.